

1
2
3
4
5
6

Design and Simulation of PDMS and PMMA Based Touch Mode Capacitive Pressure Sensor: A Comparative Study

10
11
12
13
14
15

ABSTRACT

Aims: In this research work, a design method and a comparative of a touch mode capacitive pressure sensor (TMCPs) using poly-dimethyl-siloxane (PDMS) and poly-methyl methacrylate (PMMA) is the done. A novel method is proposed to linear the output characteristics of the sensor because planer type capacitive sensors are non-linear.

Study design: This method uses a mechanical coupler to convert the deflection of the diaphragm into a linear displacement that helps to linear the output characteristics. The mathematical model of the sensor is designed and simulated the 3D model to validate the mathematically calculated values.

Place and Duration of Study: This study is done in the Department of Electronics and Communication Engineering, Rajiv Gandhi University, Arunachal Pradesh at COMSOL Simulation Laboratory during 2021 to 2023.

Methodology: The mechanical and electrostatic components of the sensor are represented mathematically model in two separate parts. For this study, a square diaphragm was used since it exhibits greater deflection than circular or rectangular diaphragms. In order to validate the model equation, a 3D model of a sensor is created in the COMSOL Multiphysics simulator and simulated. For the pressure range of 0.1 [MPa] to 10.1 [MPa], the identical 3D model of the sensor construction with a square diaphragm thickness of 20 μm is simulated for PDMS and PMMA. The different elements influencing the sensor's sensitivity are discovered, and the effects of the materials PDMS and PMMA on the output characteristic are discussed.

Results: The simulated and calculated sensitivity of the sensors based on PDMS are 0.03685 [fF/MPa] and 0.03467 [fF/MPa] respectively. And the simulated and calculated sensitivity of the sensors based on PMMA are 0.03929 [fF/MPa] and 0.03748 [fF/MPa] respectively. It is observed that the PDMS based TMCPs has more sensitivity then the PMMA based TMCPs.

Conclusion: The PMMA based TMCPs has higher sensitivity than the PDMS based TMCPs. The various parameters that affect the sensitivity of the sensor are diaphragm shape, size, Poisson's ratio and Young's modulus, area covered by the dielectric material, dielectric constant of the polymers dielectric and surface are of the electrode plate.

Future Scope: Future research for TMCPs can be conducted using composite polymer dielectric materials and new polymer dielectric materials to improve the sensitivity. One can optimize the sensor using different tools as the mathematical model is developed.

16
17

Keywords: Linear, Mechanical Coupler, Planer, Touch-mode, Sensitivity.

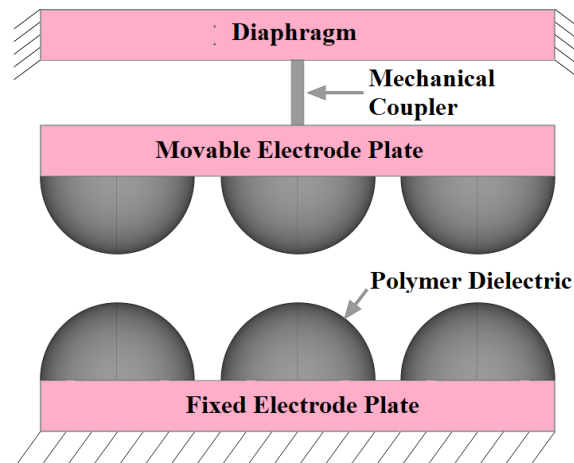
18

19 1. INTRODUCTION

20

21 There are different types of pressure sensors based on the physical sensing mechanisms,
22 they are piezoelectric, piezoresistive, inductive, capacitive, untrasonics etc [1-5]. All these
23 sensor also used in different application like turbulence flow sensing, mass colloidal flow
24 sensing, wearables sensor, electronics skins [5-8][13]. There are three main types of
25 capacitive pressure sensors. They are planar capacitive pressure sensors, comb structure
26 capacitive pressure sensors, and touch mode capacitive pressure sensors [9-13][20]. In
27 planar capacitive pressure sensor, the diaphragm structure does not come in contact with
28 the bottom electrode plate, which is fixed. Such sensor is having lower sensitivity than the
29 touch mode capacitive and they are nonlinear output with the input pressure. In touch mode
30 capacitive pressure sensor, the diaphragm structure comes into contact with the dielectric
31 which is attached to the bottom electrode plate. Such sensors provide a number of benefits,
32 including a nearly linear output to input pressure relationship, a broad input range, and a
33 robust design that can endure harsh environments. Polymers are employed as the dielectric
34 in touch mode capacitive because they may bend under increased pressure and restore
35 their original shape after the pressure is released. Polymers are widely used in touch mode
36 capacitive pressure sensor. Not all polymers are ineligible for use in touch mode capacitive
37 pressure sensors because some polymers also exhibit thermoplastic, pyroelectric, and
38 piezoelectric properties, such as PVDF and PVDF composite[17-18]. With the proper
39 packing, this sensor can be used to measure fluid flow, acceleration, and force. In comb
40 structure capacitive pressure sensor, this sensor structure has interdigitated fingers that
41 resemble two combs interlocking. This sensor structure had a larger surface area than the
42 planar and touches mode structure, which enhanced the sensor capacitance. The comb
43 structure capacitive pressure sensor has two modes of operation, transverse and
44 longitudinal. This kind of sensor has high sensitivity by nonlinear output characteristic.
45 The output of a simple touch mode capacitive pressure sensor is nonlinear because the
46 diaphragm deformed parabolically their structure while applying the pressure [8][11][19],
47 therefore a modified touch mode capacitive pressure sensor with a mechanical coupler is
48 proposed as shown in fig. 1. The mechanical coupler will transform the nonlinear
49 deformation of the diaphragm plate into a linear displacement which will produce linear
50 output characteristic.

51

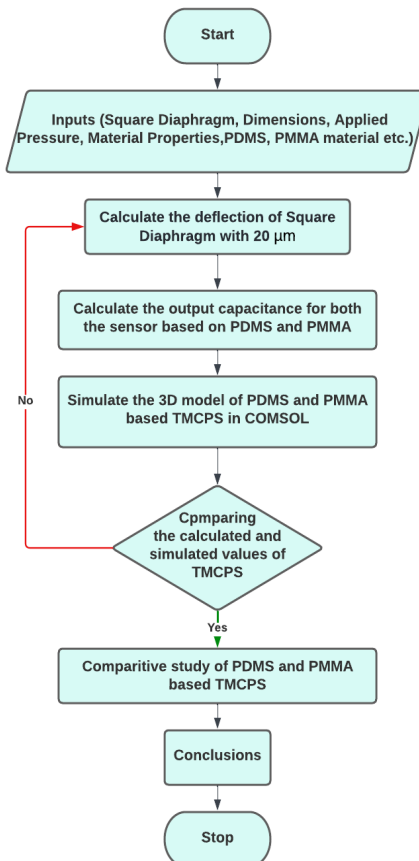


52 Fig. 1: Modified structure of TMCP.

53 The proposed structure has a diaphragm, mechanical coupler, movable plate, polymer
54 dielectric and fixed plate. In the diaphragm, the pressure is applied and deflects. This
55 deflection is converted in linear displacement by mechanical coupler which is attached
56 between the diaphragm and movable plate. The movable plate moves toward the fixed plate
57 which is separated by polymer. This polymer dielectric keeps the moveable plate away from
58 touching the fixed plate.
59

60 2. MATERIAL AND DESIGN METHODOLOGY

61
62 The suggested approach measures the deflection of square diaphragms over a pressure
63 range of 0.1 [MPa] to 10.1 [MPa] with step size 1 [MPa] in order to calculate the output
64 capacitance of the modified TMCPS. The 3D modelsof TMCPS are proposed with the
65 following specifications: the hemispheres ofPDMS and PMMA dielectric polymers with a
66 radius of 40 [μm], the square diaphragm with a length of 300 [μm] and a thickness of 20
67 [μm], and the square capacitor plates with a length of 300 [μm] and a thickness of 20 [μm].
68 The deflection of the square diaphragm is calculated for the applied pressure then the output
69 capacitances of the TMCPS based on PDMS and PMMA based TMCPS is calculated. The
70 proposed 3D model is simulated with two different types of polymer dielectrics i.e., PDMS
71 and PMMA. The verification of simulated and calculated values is done twice, one with the
72 PDMS based sensor and another is with the PMMA based sensor.



73
74

Fig. 2: The proposed methodology of design flow.

75 A comparative study is carried out between the two sensors, one with the PDMS based
 76 sensor and another with the PMMA based sensor. After conducting a comparison analysis, a
 77 number of significant findings were drawn from the various observations. The proposed
 78 methodology of design flow is shown in fig. 2.

79 The touch mode capacitive pressure sensor is similar to other Micro-Electro-Mechanical
 80 systems. This typically consists of two parts: the mechanical and electrostatic parts. Hence,
 81 mechanical and electrostatic components are mathematically calculated in accordance with
 82 their respective operating principles.

83 In mechanical model, the diaphragm converts the applied pressure into the deflection. This
 84 deflection is converted into linear displacement by the mechanical coupler. For calculating
 85 the deflection of the square diaphragm, let us consider a rectangular diaphragm with a
 86 length of $2b$ which is in y -direction and breadth of $2a$ which is in x -axis. The total energy Ω
 87 of the rectangular diaphragm for applied pressure P is given as follow [14-16].
 88

$$89 \quad \Omega = \frac{D}{2} \int_{-b}^b \int_{-a}^a \left\{ \left(\frac{\partial^2 \psi(x,y)}{\partial x^2} + \frac{\partial^2 \psi(x,y)}{\partial y^2} \right)^2 - (1-\nu) \left\{ \frac{\partial^2 \psi(x,y)}{\partial x^2} \frac{\partial^2 \psi(x,y)}{\partial y^2} - \left(\frac{\partial^2 \psi(x,y)}{\partial x \partial y} \right)^2 \right\} \right\} dx dy - \int_{-b}^b \int_{-a}^a \psi(x,y) P dx dy, \quad (1)$$

90 Where, $\psi(x,y)$ = deflection function, D = flexural rigidity and ν = Poisson's Ratio. The value of
 91 D is given by

$$92 \quad D = \frac{Eh^3}{12(1-\nu^2)} \quad (2)$$

93 Where, h = thickness of the diaphragm and E = Young's Modulus. The deflection function
 94 $\psi(x,y)$ of a rectangular diaphragm is given by [15-16]

$$95 \quad \psi(x,y) = \omega(a^2 - x^2)^2 (b^2 - y^2)^2, \quad (3)$$

96 Where ω = constant. From Eq.1 and Eq. 3 and applying the condition $\frac{\partial \Omega}{\partial \omega} = 0$, we get

$$97 \quad \omega = \frac{49P}{128(7a^4 + 4a^2b^2 + 7b^4)D} \quad (4)$$

98 Putting the value of ω into Eq. 3, The Eq. 3 becomes

$$99 \quad \psi(x,y) = \frac{49P}{128D(7a^4 + 4a^2b^2 + 7b^4)} (a^2 - x^2)^2 (b^2 - y^2)^2 \quad (5)$$

100 The side length of the square diaphragm is equal i.e., $a=b$, then Eq. 5 becomes

$$101 \quad \psi(x,y) = 0.02126 \frac{Pa^4}{D} \left(1 - \frac{x^2}{a^2}\right)^2 \left(1 - \frac{y^2}{a^2}\right)^2. \quad (6)$$

102 Eq. 6 is the deflection function at (x,y) point of a square diaphragm. At the centre of the
 103 diaphragm i.e. $(x,y)=(0,0)$, the maximum deflection of a square diaphragm is occurred and is
 104 given by

$$105 \quad \psi(x,y)_{\max} = \psi(0,0) = \psi = 0.02126 \frac{Pa^4}{D}$$

$$106 \quad \psi(x,y)_{\max} = \psi(0,0) = \psi = 0.25512 \frac{Pa^4}{Eh^3} (1-\nu^2) \quad (7)$$

107 From Eq. 7, the maximum deflection of the diaphragm is depending on the Poisson's ratio,
 108 Young's modulus, thickness of the diaphragm, length of the square diaphragm, and applied
 109 pressures.

110 In electrostatic modeling, fig. 1 displays a design model for the TMCPS using PDMS or
 111 PMMA as the polymer dielectric material. Hemispherical polymers are used to coat portions

112 of the electrode plates, but not all of them. The surfaces of the electrodes are separated into
 113 two sections: one section is the portion of the electrodes covered in dielectric polymers, and
 114 the other section is the remainder of the electrode surface that is uncoated.

115 As a result, the sum of capacitances C_1 and C_2 can be used to compute the overall
 116 capacitance C . Where C_1 denotes the capacitance of the dielectric polymer-covered area
 117 and C_2 denotes the capacitance of the uncovered area.

$$118 \quad C = C_1 + C_2, \quad (8)$$

119 Now, the value of C_1 and C_2 can be calculated by

$$120 \quad C_1 = n \frac{\varepsilon_0 \varepsilon_r}{(g - \psi)} \pi r^2, \quad (9)$$

$$121 \quad C_2 = \frac{\varepsilon_0 (\alpha - n\pi r^2)}{(g - \psi)}, \quad (10)$$

122 Where, r = radius of the hemisphere, n = number of hemispherical polymer dielectric, ε_0 =
 123 absolute permittivity, ε_r = relative permittivity, α = surface area covered of the electrode plate
 124 and g = gap between the electrodes. Now, the total capacitance of the TMCPS is

$$125 \quad C = \frac{\varepsilon_0 (\alpha + n\pi r^2 (\varepsilon_r - 1))}{(g - \psi)}, \quad (11)$$

126 The sensitivity of the sensor S is ratio of change in the output to the change in input.
 127 Mathematically the sensitivity can be express for TMCPS is

$$128 \quad S = \frac{\varepsilon_0 (\alpha + (\varepsilon_r - 1)n\pi r^2)}{P(g - \psi)}. \quad (12)$$

129 From Eq. 12, the sensitivity of the sensor is depending on the total area covered by the of
 130 the polymer dielectric hemisphere, surface area of the electrode, gap between electrodes,
 131 relative permittivity and all the parameters that affect the deflection i.e., Poisson's ratio,
 132 Young's modulus of the diaphragm's materials, thickness of the diaphragm, length of the
 133 square diaphragm, and applied pressures.

134 Tables should be explanatory enough to be understandable without any text reference.
 135 Double spacing should be maintained throughout the table, including table headings and
 136 footnotes. Table headings should be placed above the table. Footnotes should be placed
 137 below the table with superscript lowercase letters.

138

139 **3. RESULTS AND DISCUSSION OF SIMULATED 3D MODEL OF TMCPS**

140 The COMSOL Multiphysics simulator was used to simulate the 3D model of the TMCPS
 141 based on PDMS and PMMA, which is depicted in fig. 1. This model contains a square
 142 diaphragm, mechanical coupler, moving electrode plate, fixed electrode plate, and a
 143 numbers of hemisphere-shaped dielectric polymers. The mechanical coupler is used to
 144 transform the deflection into linear displacement. Table 1 tabulates the physical dimension of
 145 the various TMCPS components, while table 2 tabulates the material properties of TMCPS
 146 components.

147 **Table 1: Physical dimension of the TMCPS's components.**

TMCPS Components	Material	Dimensions		
		Length	Breath	Thickness/ Radius
Diaphragm	Gold	300 [μm]	300 [μm]	20 [μm]
Mechanical Coupler	Silicon-dioxide	20 [μm]	20 [μm]	20 [μm]

Electrode Plates	Gold	300 [μm]	300 [μm]	20 [μm]
Polymer Dielectric	PMMA/PDMS	-	-	40 [μm]

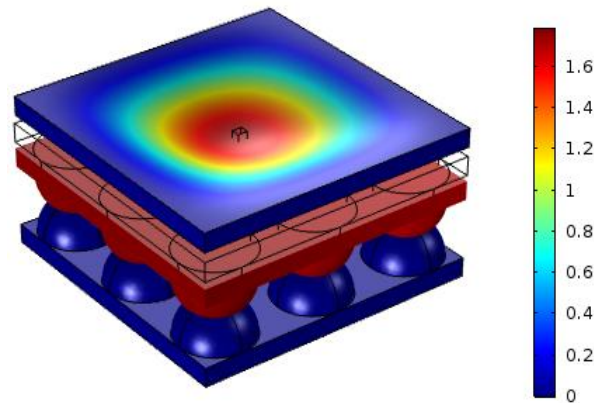
148

149 **Table 2: Material properties of the TMCPS components.**

Material	Young's modulus	Poisson's ratio	Dielectric Constant
Gold	70 [GPa]	0.425	-
Silicondioxide	70 [GPa]	0.17	-
PDMS	-	-	2.4
PMMA	-	-	3

150

151 After designing the 3D model of the TMCPS in the COMSOL simulator, the material
 152 properties of the various components are defined in the simulator. The mechanical and
 153 electrostatic are configured and the applied pressure is also defined in the global variable. A
 154 parametric swap is done in COMSOL for input pressure starting from 0.1 [MPa] to 10.1
 155 [MPa] with a step size of 1 [MPa].



156

157 **Fig. 3: COMSOL simulation output showing the deflection and shifting of movable**
 158 **electrode plate.**

159 In table 3, the deflection values that were calculated and simulated for both PDMS and
 160 PMMA based TMCPS are listed. The deflection is same for all both the sensors as the
 161 diaphragm is of same material for both the sensor. Also, it has been found that as increases
 162 in applied pressure, the deflection increases also increase.

163 **Table 3: Calculated and simulated values of deflections.**

Pressure [MPa]	Sim [μm]	Cal [μm]
0.1	0.01742	0.0186
1.1	0.19167	0.2046
2.1	0.3658	0.3906
3.1	0.5398	0.5766

4.1	0.7136	0.7625
5.1	0.8872	0.9485
6.1	1.0611	1.1345
7.1	1.2339	1.3205
8.1	1.4076	1.5065
9.1	1.5791	1.6924
10.1	1.7516	1.8784

164

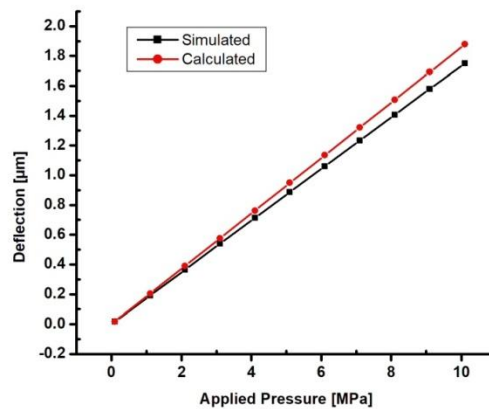
165 The simulated and calculated capacitance values for the proposed TMCPS are shown in
 166 table 4. The output capacitance is in the fF range, as can be observed from the data. The
 167 values also increase as the applied pressure is increased. The PMMA sensor has higher
 168 capacitance values than the PDMS sensor, the reason is PMMA has higher dielectric values
 169 than PDMS.

170 **Table 4: Calculated and simulated values of capacitance.**

Pressure [MPa]	PDMS-TMCPS [fF]		PMMA-TMCPS [fF]	
	Sim	Cal	Sim	Cal
0.1	16.7187	16.4263	17.1025	17.7623
1.1	16.7546	16.4603	17.1408	17.7991
2.1	16.7908	16.4945	17.1793	17.8360
3.1	16.8272	16.5288	17.2181	17.8731
4.1	16.8638	16.5632	17.2571	17.9103
5.1	16.9006	16.5978	17.2963	17.9477
6.1	16.9376	16.6326	17.3357	17.9853
7.1	16.9747	16.6674	17.3753	18.0230
8.1	17.0120	16.7025	17.4152	18.0609
9.1	17.0496	16.7377	17.4552	18.0989
10.1	17.0872	16.7730	17.4954	18.1371

171

172 The graphic representations of table 3 are shown in fig. 4. The simulated and calculated
 173 deflections are seen to linearly change with the applied pressures..



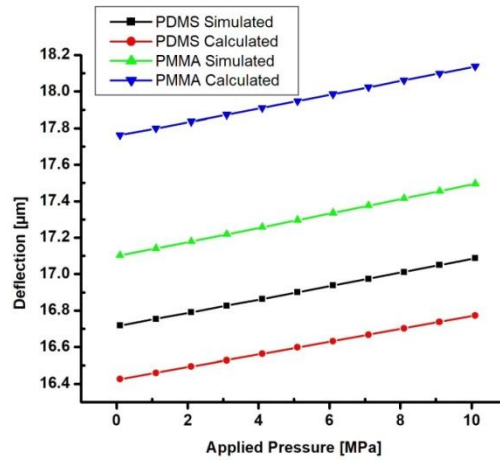
174

175 **Fig. 4: Calculated and simulated deflections values for the applied pressures.**

176

177 Additionally, it has been noted that although the calculated values and simulated values are
 177 practically identical and the calculated values are slightly higher than the simulated values.

178 So the mathematical model of the deflection can be used for further study. This linearly
 179 deflection at the center of the diaphragm is translated to linear displacement by the
 180 mechanical coupler. Because of this linear translation the output capacitance of the sensor is
 181 linear in characteristics.



182
 183 **Fig. 5: Calculated and simulated output capacitances values for the applied**
 184 **pressures.**

185 Fig. 5 illustrates is the graphical representation of table 4. The simulated and calculated
 186 values of output capacitance are also linear with those of input pressure. The simulated
 187 output values are less than the calculated values but they are much closed. The PDMS
 188 based sensor has less sensitive then the PMMA based sensor. This is because the dielectric
 189 coefficient of the PDMS is lower than the dielectric coefficient of the PMMS. As the output
 190 values are much closed we can used the proposed mathematical model of the sensor in
 191 future application. The proposed improved model of the touch mode capacitive pressure
 192 sensor is very linear compared to the nonlinear planar touch mode capacitance pressure
 193 sensors. From the mathematical model, the various factor affecting the sensitivity of the
 194 sensor can be found.

195
 196 **4. CONCLUSION**
 197

198 This research study focuses on the mathematical modeling and simulation of the touch
 199 mode capacitive pressure sensor for pressure ranges of 0.1 [MPa] to 10.1 [MPa]. A design
 200 method based on PMMA and PDMS is presented and realized for a touch mode capacitive
 201 pressure sensor. Due to the strong agreement between the simulated and calculated values,
 202 the mathematical expression can be used to find the various factors impacting on the
 203 sensitivity of the sensors. The deflection if the diaphragm is increases with the applied
 204 pressure and surface area of the diaphragm. The deflection of the diaphragm is decrease
 205 with increase in Young's modulus, thickness of the diaphragm and Poisson's ratio as it has
 206 negative values. The output capacitances are increase with increase in deflection, area
 207 covered by the dielectric materials and relative permittivity of the dielectric but decrease
 208 with increase in the gaps between the two electrode plates. The non linear deflection is finally
 209 converted into linear displacement by a mechanical coupler to produce a sensor with a linear
 210 output characteristic. The sensitivity of the PDMS-based touch mode capacitive pressure for
 211 simulated and calculated data for a 20 [µm] diaphragm thickness is 0.03685 [fF/MPa] and
 212 0.03467 [fF/MPa], respectively. The sensitivity of the PMMA-based touch mode capacitive

213 pressure is 0.03929 [fF/MPa] for simulated pressure and 0.03748 [fF/MPa] for calculated
214 pressure for a 20 [µm] thick diaphragm. The sensitivity of the PMMA based TMCPS is higher
215 than the PDMS based TMCPS.

216
217

218 **COMPETING INTERESTS**

219

220 “Authors have declared that no competing interests exist”.

221

222 **AUTHORS’ CONTRIBUTIONS**

223

224 ‘Maibam Sanju Meetei’ designed the mathematical model and simulation of this work, and
225 wrote the first draft of the manuscript. ‘Heisnam Shanjit Singh’ managed the analyses of the
226 study and wrote the second draft of the manuscript. Then both the authors read and
227 approved the final manuscript.”

228

229 **REFERENCES**

230

231 1. Chen D., Cai Y., Huang M. C. Customizable Pressure Sensor Array: Design and
232 Evaluation. IEEE Sensors Journal. 2018;18(15):6337-6344.

233 2. Yang W., Yang Q., Yan R., Zhang W., Yan X., Gao F., Yan W. Dynamic Response of
234 Pressure Sensor With Magnetic Liquids. IEEE Transactions on Applied
235 Superconductivity. 2010;20(3):1860-1863.

236 3. Li L., Wang L., Qin L., Lv Y. The theoretical model of 1-3-2 piezocomposites. IEEE
237 Transactions on Ultrasonics, Ferroelectrics, and Frequency Control, 2009;56(7):1476-
238 1482.

239 4. Shu L., Tao X., Feng D. D. A New Approach for Readout of Resistive Sensor Arrays for
240 Wearable Electronic Applications. IEEE Sensors Journal. 2015;15(1):442-452.

241 5. Bakhom E. G., Cheng M. H. M. High-Sensitivity Inductive Pressure Sensor. IEEE
242 Transactions on Instrumentation and Measurement. 2011;60(8):2960-2966.

243 6. Houri C. G., Talbi A., Viard R., Gallas Q., Garnier E., Molton P., Delva J., Merlen A.,
244 Pernod, P. Robust thermal microstructure for designing flow sensors and pressure
245 sensors. In Proceedings of the 2017 IEEE Sensors. 2017:1-3.

246 7. Bera S. C., Mandal N., Sarkar R. Study of a Pressure Transmitter Using an Improved
247 Inductance Bridge Network and Bourdon Tube as Transducer. IEEE Transactions on
248 Instrumentation and Measurement. 2011;60(4):1453-1460.

249 8. Luo J., Zhang L, Wu T., Song H., Tang C. Flexible piezoelectric pressure sensor with
250 high sensitivity for electronic skin using near-field electrohydrodynamic direct-writing
251 method. Extreme Mechanics Letters. 2021;48:101279.

252 9. Houri C. G., Talbi A., Viard R., Gallas Q., Garnier E., Molton P., Delva J., Merlen A.,
253 Pernod P. MEMS high temperature gradient sensor for skin-friction measurements in
254 highly turbulent flows. In Proceedings of the 2019 IEEE Sensors. 2019: 9749 – 9755.

* Tel.: +91 94 36069533.

E-mail address: maibamkhuman@gmail.com

- 255 10. Alveringh D., Schut T. V. P., Wiegerink R. J., Sparreboom W., Lötters J. C. Resistive
256 pressure sensors integrated with a coriolis mass flow sensor. In Proceedings of the 19th
257 International Conference on Solid-State Sensors, Actuators and Microsystems
258 (TRANSDUCERS).2017:1167-1170.
- 259 11. Meetei M. S., Singh H. S., Singh A. D., Majumder S. A novel design and optimization for
260 beam bridge piezoelectric pressure sensor. 2020;11(12):2687-2701.
- 261 12. Meetei M. S., Singh H. S. Modelling and Simulation of a Diaphragm based Touch Mode
262 Capacitive Pressure Sensor (DTMCPS). International Journal of Mechanical
263 Engineering. 2021;6(3):2784-2788.
- 264 13. Cotton D. P. J., Graz I. M., Lacour S. P. A Multifunctional Capacitive Sensor for
265 Stretchable Electronic Skins. IEEE Sensors Journal. 2009;9(12):2008-2009.
- 266 14. Timoshenko S. P., Woinowsky-Krieger, S. Theory of Plates and Shells. Mc Graw Hill;
267 New York:1959.
- 268 15. Ugural A. C. Plates and shells: theory and analysis. Boca Raton: London New York;
269 2018.
- 270 16. Bao M. Analysis and Design Principles of MEMS Devices. Elsevier Science: Amsterdam
271 Netherlands;2005.
- 272 17. Anshuman Srivastava, PralayMaiti, Devendra Kumar, Om Parkash. Mechanical and
273 dielectric properties of $\text{CaCu}_3\text{Ti}_4\text{O}_{12}$ and La doped $\text{CaCu}_3\text{Ti}_4\text{O}_{12}$ poly(vinylidene fluoride)
274 composites. Composites Science and Technology 2014;93:83–89.
- 275 18. Anshuman Srivastava, Karun Kumar Jana, Pralay Maiti, Devendra Kumar and Om
276 Parkash. Poly(vinylidene fluoride)/ $\text{CaCu}_3\text{Ti}_4\text{O}_{12}$ and La doped $\text{CaCu}_3\text{Ti}_4\text{O}_{12}$ composites
277 with improved dielectric and mechanical properties. Material Research
278 Bulletin.2015;70:735-742.
- 279 19. Sumit Kumar Jindal, M. Aditya Varma, Deepali Thukral. Comprehensive assessment of
280 MEMS double touch mode capacitive pressure sensor on utilization of SiC film as
281 primary sensing element: Mathematical modelling and numerical simulation.
282 Microelectronics Journal. 2018;73:30-36.
- 283 20. Sanghwa Hong, Seongkook Heo, Byungjoo Lee. MaterialSense: Estimating and utilizing
284 material properties of contact objects in multi-touch interaction. International Journal of
285 Human-Computer Studies. 2023;172:102985.

* Tel.: +91 94 36069533.

E-mail address: maibamkhuman@gmail.com